



Contents lists available at ScienceDirect



Catalysis Today

journal homepage: www.elsevier.com/locate/cattod

NiW/MgO–TiO₂ catalysts for dibenzothiophene hydrodesulfurization: Effect of preparation method

Alida Elizabeth Cruz Pérez ^{a,*}, Yesenia Torrez Jiménez ^a, Jessica Joana Velasco Alejo ^a, Trino A. Zepeda ^b, Dora María Frías Márquez ^a, María Guadalupe Rivera Ruedas ^a, Sergio Fuentes ^b, Jorge Noé Díaz de León ^b

^a División Académica de Ingeniería y Arquitectura, Universidad Juárez Autónoma de Tabasco, Carretera Cunduacán-Jalpa de Méndez Km 1, C.P. 86690, Mexico

^b Universidad Nacional Autónoma de México, Centro de Nanociencias y Nanotecnología, Carretera Tijuana-Ensenada Km 107, C.P. 22800, Mexico

ARTICLE INFO

Article history:

Received 8 April 2015

Received in revised form 22 July 2015

Accepted 28 July 2015

Available online xxxx

Keywords:

MgO–TiO₂ mixed-oxides

Hydrodesulfurization

Dibenzothiophene

Active phases

WS₂-crystallites

ABSTRACT

In the present work NiW-based catalysts supported on binary MgO–TiO₂ mixed oxides (MT-x, where x is the mol% of TiO₂) were prepared by aqueous and non-aqueous methods. The results from the characterization techniques (N₂ adsorption/desorption, XRD, UV-vis DRS and HRTEM) were used to establish a relationship between the preparation method and the structural changes of W phases as well the catalytic activity. N₂ adsorption/desorption isotherms showed higher surface areas with the increase on mol% of TiO₂. Catalysts characterization showed that the preparation method did not change the original structure of the supports. Furthermore, the presence of NiO and NiWO₄ was not observed in any sample, thus, the supports allowed a good dispersion of Ni and W species. DRS spectra showed the presence of W⁶⁺ in octahedral coordination and tetrahedral Ni²⁺. Correlation of the catalytic activity in the DBT HDS reaction and the fraction of W atoms on the edge of WS₂ crystallites indicated that the aqueous impregnation on MT25, followed by drying at 393 K leads to the formation of a greater number of catalytically active sites available for interaction with DBT molecules.

© 2015 Elsevier B.V. All rights reserved.

1. Introduction

Hydrodesulfurization process is of paramount importance, since oil products must be purified to diminish air-polluting emissions of sulfur oxides, which contribute to acid rain. Thus, many oil streams in a refinery must therefore treated by the process of hydrodesulfurization (HDS) [1]. In this context, deep fuel HDS implies full removal of the refractory sulfur compounds, such as dibenzothiophenes, alkylbenzothiophenes and alquildibenzothiophenes [2]. Typically the catalytic activity is carried out over materials containing MoS₂ (WS₂) nanoslabs promoted by Co or Ni and supported on γ-Al₂O₃. Topsoe et al. [3] named these structures as non-stoichiometric “CoMoS” and “NiWS” phases, as suggested by Topsoe et al. [3]. The CoMoS phase was shown to be MoS₂-like structures with the promoter (Co or Ni) atoms located at edge planes of MoS₂ in five-fold coordinated sites [3]. Moreover, these authors claim that a single slab structure (called Type I Co-Mo-S) interacts strongly with the support, probably via Mo–O–Al linkages located

at the edges on alumina-supported catalysts, whereas for the multiple slab (called Type II Co-Mo-S) these interactions are smaller [3].

Industrial hydrodesulfurization uses bimetallic catalysts based on Mo/W, promoted by Ni/Co and supported on γ-Al₂O₃. It is well known that the nature of the support plays an important role to improve the HDS activity. For example, it has been found that titania supported CoMo catalysts have 1.9 times the HDS activity of their alumina counterparts [4]. In this line, modification of hydrodesulfurization catalysts by incorporation of acid and basic supports has been performed [5]. Basic supports allow a high and stable dispersion of catalytically active Mo species. Besides, a basic support could inhibit the coke formation [6]. Researchers found that MoS₂ supported on MgO is more active in dibenzothiophene (DBT) HDS than when it is supported on Al₂O₃, the enhanced activity was attributed to high Mo dispersion on MgO support [7,8]. In literature, there are several studies about the activity of catalysts supported on MgO–Al₂O₃ in HDS [9,10]. However, some works reported the loss of HDS activity with catalysts NiMo supported on MgO–Al₂O₃ mixed oxides, due to the formation of solid NiO–MgO solution and MgMoO₄ spinel during aqueous impregnation [11–13]. Aqueous impregnation of Ni and Mo on MgO presents serious problems,

* Corresponding author.

E-mail address: alidaelizabeth2009@hotmail.com (A.E. Cruz Pérez).

the high MgO surface area allows a reaction with water leading to Mg(OH)₂ formation [14]. In order to solve this problem Zdrazil et al. [15] propose the use of organic solvents such as dimethylsulphoxide and methanol. Apparently, the textural properties of MgO are stable with these solvents. However, (NH₄)₆Mo₇O₂₄ and Ni(NO₃)₂ solubility in those solvents is very low, which complicates the conventional impregnation process. On the other hand, a number of papers report on the role of additives in the sintering of MgO [16–18]. Additions of tetravalent Si, Ti and Zr enhance sintering. Thereby, some authors reported that the addition of TiO₂ promotes MgO densification and grain growth at relative low temperature [19]. Furthermore, the mixing of solid oxides produces systems that have novel acid or basic properties. These properties can be modified varying their mixing concentration. In the MgO–SiO₂ system, which has a basic behavior, its basicity strongly depends on MgO content [20,21] being maximal for 50 wt% MgO. TiO₂–MgO mixed oxide shows a basic behavior [22]. The substitution of titanium ions for magnesium ions in magnesia lattice. This deforms magnesia crystalline structure and produces unbalanced electron charges [22], thus it contributes to the basicity observed in these materials. In the present work, two series of NiW catalysts supported on MgO–TiO₂ were synthesized, they were impregnated by aqueous and non-aqueous methods. The aim of this work is to explore the effect of the solvent used for impregnation on the stability of the support MgO–TiO₂(x) during the preparation and activation of NiW/MgO–TiO₂ catalysts and consequently on the activity in HDS of DBT.

2. Experimental

2.1. Preparation of MgO–TiO₂ supports

MgO–TiO₂ supports with 10, 25 and 50 mol% of TiO₂ were prepared by sol–gel method [23]. Magnesium ethoxide and titanium isopropoxide (Aldrich-Chemical ≥75%) were dissolved into methanol and 2-propanol respectively (1 g alcoxide/100 mL alcohol). Then, both solutions were mixed and stirred during 4 h at 343 K. The gel was obtained by hydrolysis with dropwise addition of deionized water. Then, the gel was dried at 393 K for 12 h and then calcined at 823 K for 6 h. Nomenclature for supports: MT10 for 10 mol% TiO₂; MT25 for 25 mol% TiO₂ and MT50 for 50 mol% TiO₂.

2.2. Synthesis of NiW/MgO–TiO₂ catalysts

In order to obtain catalyst with 26 wt.% WO₃ and 4 wt.% NiO, the support (100–150 mesh) was co-impregnated, using the incipient wetness method, with a solution of ammonium metatungstate (NH₄)₆W₁₂O₃₉·H₂O (Aldrich ≥65%) and nickel nitrate Ni(NO₃)₂·6H₂O (Aldrich ≥70%) using H₂O as solvent for aqueous impregnation and methanol for non-aqueous impregnation. After 12 h, the obtained solids were dried at 393 K for 10 h and calcined at 673 K for 4 h. The solids were characterized and evaluated, before and after the calcination process. Nomenclature for catalysts is shown in Table 1.

2.3. Characterization of the solids

Surface area, pore volume, and pore size distribution of the supports and catalysts were obtained from N₂ adsorption/desorption isotherms using the conventional BET and BJH methods. The samples were outgassed at 573 K under vacuum. Afterwards, the N₂ adsorption measurements were carried out at 73 K. XRD patterns were recorded in the 20° ≤ 2θ ≤ 80° range on a Phillips X'Pert diffractometer using CuKα radiation ($\lambda = 1.5406 \text{ \AA}$) and a goniometer speed of 1°(2θ) min⁻¹. UV-vis spectra of the samples were

Table 1
Nomenclature of prepared catalysts.

| Catalyst | Mol% TiO ₂ | Impregnation method | Treatment |
|--------------|-----------------------|---------------------|-----------|
| NiW/MT10-AD | 10 | Aqueous | Dried |
| NiW/MT25-AD | 25 | Aqueous | Dried |
| NiW/MT50-AD | 50 | Aqueous | Dried |
| NiW/MT10-NAD | 10 | Non-aqueous | Dried |
| NiW/MT25-NAD | 25 | Non-aqueous | Dried |
| NiW/MT50-NAD | 50 | Non-aqueous | Dried |
| NiW/MT10-AC | 10 | Aqueous | Calcined |
| NiW/MT25-AC | 25 | Aqueous | Calcined |
| NiW/MT50-AC | 50 | Aqueous | Calcined |
| NiW/MT10-NAC | 10 | Non-aqueous | Calcined |
| NiW/MT25-NAC | 25 | Non-aqueous | Calcined |
| NiW/MT50-NAC | 50 | Non-aqueous | Calcined |

recorded in the wavelength range 200–900 nm using AvaSpec-2048 spectrophotometer equipped with a diffuse reflectance attachment. Sulfided catalysts were characterized by high resolution transmission electron microscopy (HRTEM). HRTEM studies were performed using a JEOL-JEM-2010 microscope. The solids were ultrasonically dispersed in 2-propanol and the suspension was collected on carbon coated grids. Slab length and layer stacking distributions of WS₂ crystallites in each sample were established from the measurement of at least 300 crystallites detected on several TEM micrographs taken from different parts of the sample dispersed on the microscope grid.

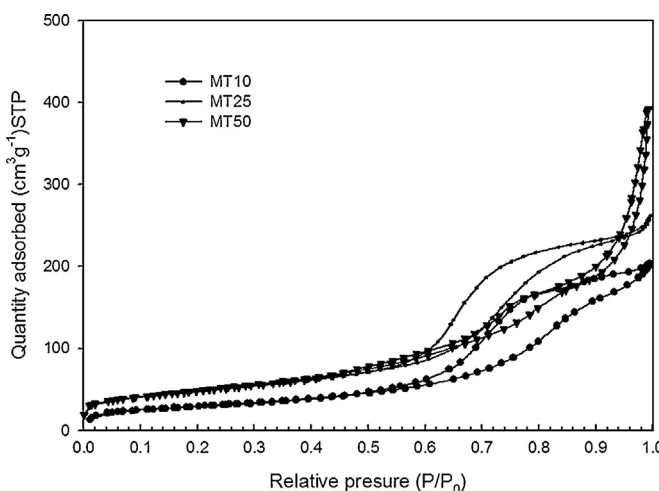
2.4. Catalytic activities measurements

The HDS of DBT was performed in a 500 mL batch reactor, magnetically stirred (700 rpm) (Parr Instrument Co.). The conditions of the tests were as follows: temperature of 593 K under a hydrogen atmosphere of 5 MPa for 8 h, using 200 mg of presulfidized catalyst and 1.25 × 10⁻³ mol of DBT dissolved in 100 mL hexadecane (Aldrich-Chemical). Before each reaction, the catalysts were activated by ex situ sulfidation in a U-shape glass flow reactor. First, the sample was flushed in a nitrogen flow and gradually increased the temperature up to 423 K. After reaching this temperature the flow was switched to the sulfidation mixture (H₂/H₂S 15 vol% H₂S) with a flow of 40 mL min⁻¹ and then increased the temperature up to 673 K in ca. 2.5 h. The sulfidation continued under these conditions for 2 h. Then the sample was cooled down to room temperature, changing the sulfidation mixture to nitrogen when the temperature decreased to 423 K. The sulfided sample was carefully transferred to the reactor in an argon atmosphere with the aim to avoid contact with air. Then the reactor was flushed with nitrogen and heated under stirring to reach the reaction temperature, hydrogen was then introduced ($P_{\text{Tot}} = 5 \text{ MPa}$). The reaction time was counted from this moment. The total pressure was controlled constantly during the course of reaction by adding hydrogen to compensate for its consumption. Samples were periodically collected and analyzed quantitatively by gas chromatography. The catalytic activity was expressed by the initial reaction rate (mol DBT transformed per second and per gram of catalyst).

3. Results and discussion

3.1. Supports and catalysts characterization

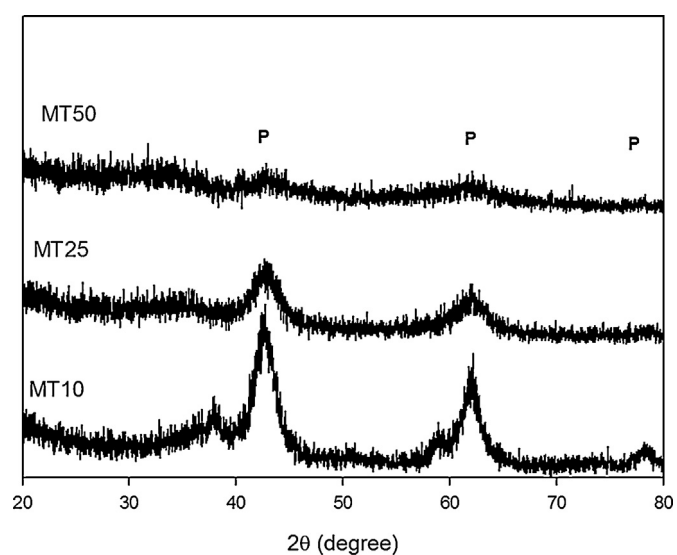
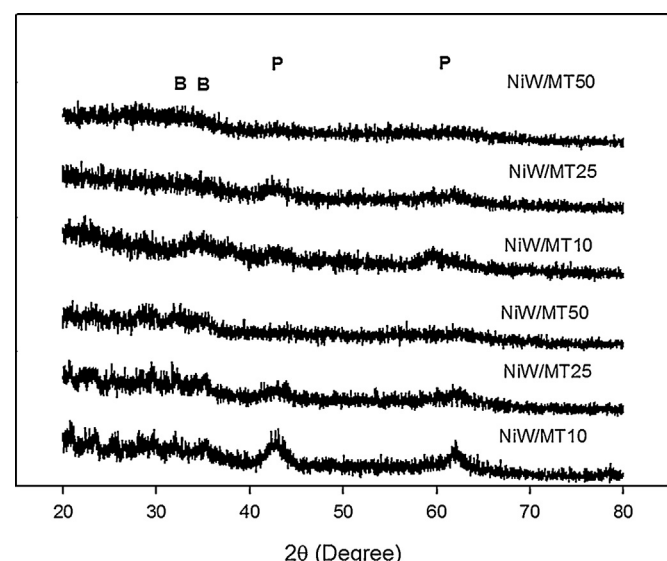
Textural properties for the supports and catalysts were determined by N₂ physisorption. Fig. 1 shows nitrogen adsorption–desorption isotherms of the supports synthesized. According to IUPAC classification, the MT10 and MT25 supports showed isotherm type IV, while it was type III when the samples had 50 mol% of titania, in agreement with the reported in another work [21]. For the three mixed oxides the pore size distribution was

Fig. 1. N_2 adsorption–desorption isotherms of $\text{MgO}-\text{TiO}_2$ supports.**Table 2**
Textural properties of supports and NiW catalysts.

| Sample | S_{BET} ($\text{m}^2 \text{ g}^{-1}$) | V_p ($\text{cm}^3 \text{ g}^{-1}$) | D_p (nm) |
|--------------|--|--|------------|
| MgTi10 | 100 | 0.29 | 7 |
| MgTi25 | 166 | 0.38 | 7 |
| MgTi50 | 181 | 0.56 | 11 |
| NiW/MT10-AD | 70 | 0.13 | 7 |
| NiW/MT25-AD | 117 | 0.16 | 5 |
| NiW/MT50-AD | 36 | 0.10 | 14 |
| NiW/MT10-NAD | 70 | 0.14 | 8 |
| NiW/MT25-NAD | 66 | 0.13 | 7 |
| NiW/MT50-NAD | 41 | 0.12 | 6 |
| NiW/MT10-AC | 145 | 0.28 | 6 |
| NiW/MT25-AC | 126 | 0.23 | 6 |
| NiW/MT50-AC | 57 | 0.15 | 11 |
| NiW/MT10-NAC | 105 | 0.30 | 9 |
| NiW/MT25-NAC | 96 | 0.21 | 6 |
| NiW/MT50-NAC | 82 | 0.19 | 10 |

bimodal. The BET area and pore diameter changed in the following trend: MT50 > MT25 > MT90 (Table 2). Since the TiO_2 shows an $S_{\text{BET}} \approx 10 \text{ m}^2 \text{ g}^{-1}$ [24], from these results we concluded that TiO_2 is a textural promoter for magnesia. Thus, the textural properties of the mixed oxides depend mainly on the relative concentration of their components, as it was reported somewhere else [23]. Results from the textural characterization (S_{BET} , V_p and D_p) of the catalysts are shown in Table 2. In general, textural characteristics of all NiW catalysts were lower than those of the corresponding supports. A comparison of the obtained results indicates that deposition of Ni and W species resulted in a decrease in the textural characteristics of the support. These findings can be explained by the mechanism of metals deposition during the impregnation process: the Ni and W species fills in the pores of high-surface area supports, diminishes their diameter and fully blocks the majority of them. Such a process can lead to a decrease in the volume of small pores and eventually, to a decrease of the surface area [25]. However, it is widely known that the presence of foreign ions could inhibit the sintering during the calcination of hydroxides to oxides [26]. From this approach, the stabilizing effect caused by the presence of anions W during hydration of MgO to Mg(OH)_2 and then in the $\text{MgO}-\text{TiO}_2$ restructuring after calcination, may explain the increased S_{BET} values of the catalysts with the highest amount of MgO , NiW/MT10-AC and NiW/MT10-NAC with respect to the starting MT10, Table 2, these results are in agreement with those reported by Zdražil [27].

Fig. 2 shows XRD patterns for the supports $\text{MgO}-\text{TiO}_2$. All of them exhibited diffraction patterns in which three well-resolved

Fig. 2. Powder XRD patterns of $\text{MgO}-\text{TiO}_2$ supports. P: periclase.Fig. 3. Powder XRD patterns of dried NiW catalysts supported on $\text{MgO}-\text{TiO}_2$. P: periclase; B: brucite.

signals can be observed: the most intense signal is situated at 42.5° (2θ) and two less intense peaks at about 68° and 36° (2θ). According to the MgO -JCPD file number 064930, these peaks can be assigned to the MgO periclase type [9,28]. Moreover the presence of any diffraction lines arising from the TiO_2 anatase phase (26° , 38° and 58° 2θ) was observed in the XRD diffraction patterns [23]. The MT50 material showed the same peaks with less intensity. This probably is due to a poor crystallinity on this sample. Which could correspond to large interactions between the crystalline phases.

Fig. 3 shows the XRD patterns of the catalysts dried. The position of the supports reflections and their intensities almost did not change after the impregnation of Ni and W species, indicating that the long-range periodicity order of the supports was preserved in the dried catalysts. The presence of small signals at 30° and 36° (2θ) were identified as Mg(OH)_2 brucite type [28], which is indicative of a surface not completely dehydroxylated [28]. These peaks were observed in catalysts impregnated by aqueous and non-aqueous methods. All signals intensity decreased in the catalysts supported on MT50.

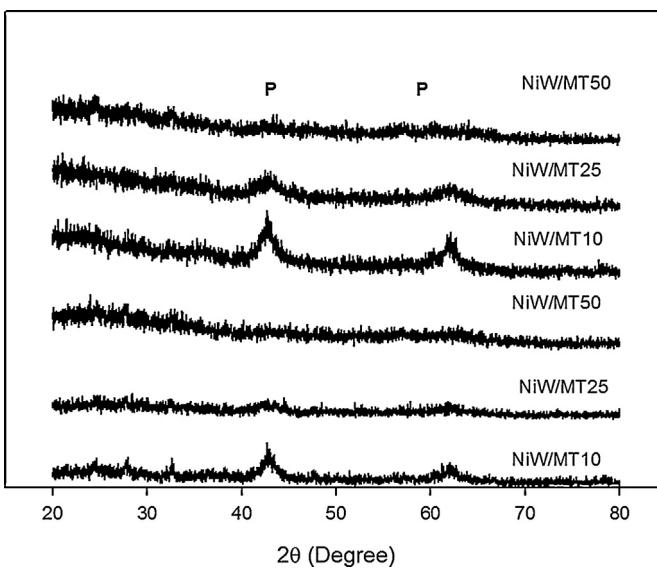


Fig. 4. Powder XRD patterns of calcined NiW catalysts supported on $\text{MgO}-\text{TiO}_2$. P: periclase.

The peaks attributed to the $\text{Mg}(\text{OH})_2$ did not appear in the XRD patterns of the calcined catalysts, Fig. 4. However, the main signals of MgO remained in the same position. Newly, the peaks intensity was lost in the catalysts supported on MT50. No signals due to the presence of any crystalline phase corresponding to the impregnated oxides such WO_3 , NiO or NiWO_4 were detected [24]. These results suggest a good dispersion of the metal oxide species present in the NiW catalysts supported on $\text{MgO}-\text{TiO}_2$. However, highly disordered (thus undetectable to the technique used) poly-tungstates domains could not be ruled out [29,30].

In literature, UV-vis diffuse reflectance (UV-vis RD) spectra for tungsten-based catalysts in the oxide state generally show 200–400 nm bands, which correspond to tungsten oxides species with tetrahedral symmetry (250–280 nm) and octahedral symmetry (290–390 nm) [31–33]. However, for $\text{MgO}-\text{TiO}_2$ supported catalysts, these bands may be overlapped with the bands caused by $\text{O}^{2-} \rightarrow \text{Ti}^{4+}$ charge transfer of TiO_2 in this region [34]. In Fig. 5, the DRS spectra of dried NiW catalysts and corresponding supports are showed. We observed a band around 250 nm, which is characteristic of TiO_2 . After impregnation, this band showed higher intensity in

the spectra of all catalysts, indicating that there may be species W^{6+} in octahedral coordination (290–390 nm). In the calcined catalysts (Fig. 6) the bands show a slight shift-blue suggesting the formation of species of W^{6+} with tetrahedral coordination (250–280 nm) during calcination.

Figs. 5B and 6B, show a broadening of the spectrum around 400–800 nm. In the spectra of all the catalyst, we observed a band at 620 nm which indicates the presence of tetrahedral Ni^{2+} . The presence of these species could be associated to the formation of Ni-support spinels [35–38].

Although supports $\text{MgO}-\text{TiO}_{2(x)}$ are stable under the conditions of aqueous and non-aqueous impregnation, Ni and W interactions with the starting supports remain unexplained from these results.

3.2. Catalytic activity in hydrodesulfurization of dibenzothiophene

Fig. 7 resumes the results obtained for the dibenzothiophene catalytic activity test. Catalysts dried impregnated by aqueous method showed the highest activity. HDS activity of catalysts calcined impregnated by non-aqueous method decreased probably, due to the low solubility of the precursor salts on methanol, thus, diminished the dispersion of the metal oxide and led to the formation of solid solutions with the support. On the other hand, it is probable that the addition of 25 mol% of TiO_2 decrease the presence of strong Ni-support interactions and allows the nickel in higher availability for the formation of the active phases, this are well exhibited by the significant increase on catalytic activity observed in the samples with low TiO_2 content (Fig. 7).

Table 3 shows the amounts of the main reaction products obtained with the dried catalysts impregnated by aqueous method. The main desulfurized product obtained with all the catalysts in the HDS of DBT was biphenyl, which points out that the DDS pathway of the reaction was the predominant reaction route. In general, the activity catalysts supported on $\text{MgO}-\text{TiO}_2$ is considerably less than that obtained with a commercial catalyst supported on Al_2O_3 . Furthermore, the selectivity of the catalysts supported on $\text{MgO}-\text{TiO}_2$ promotes direct desulfurization pathway and increases slightly with increasing TiO_2 content (HYD:DDS ratio increased). It is well known that the selectivity obtained by NiW based catalysts follows the hydrogenation pathway. This may be due to the MgO content and its basic character, the strong interaction metal– MgO could affect the number of stacks and the length of the slabs of NiWS active phases. Then, this could shift the selectivity toward

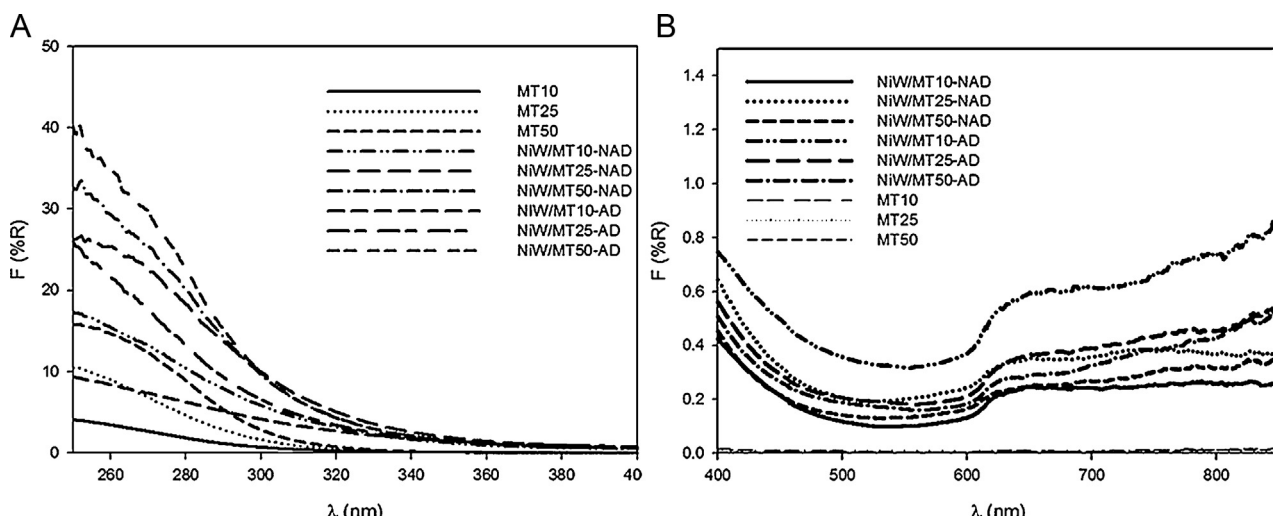
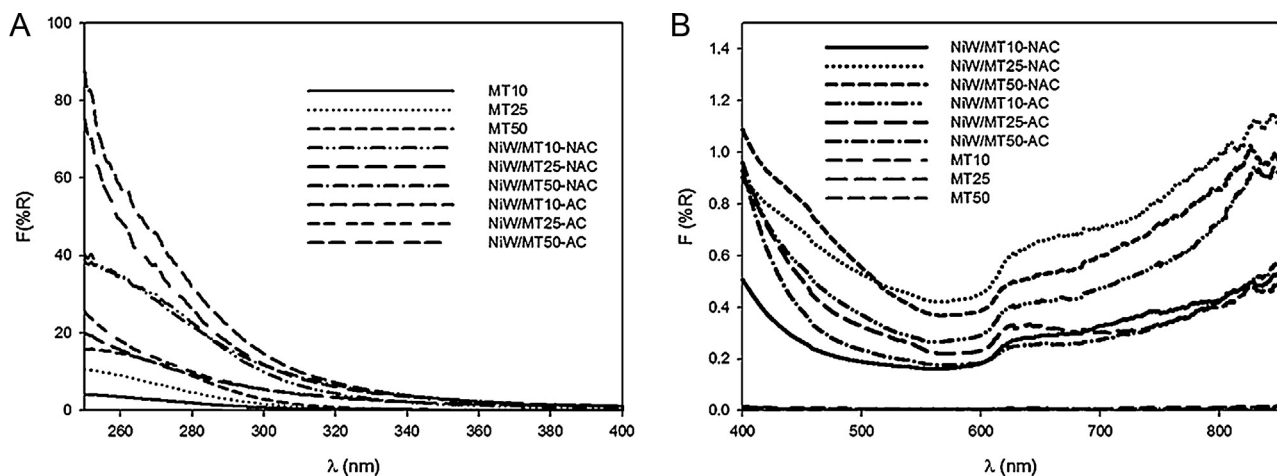
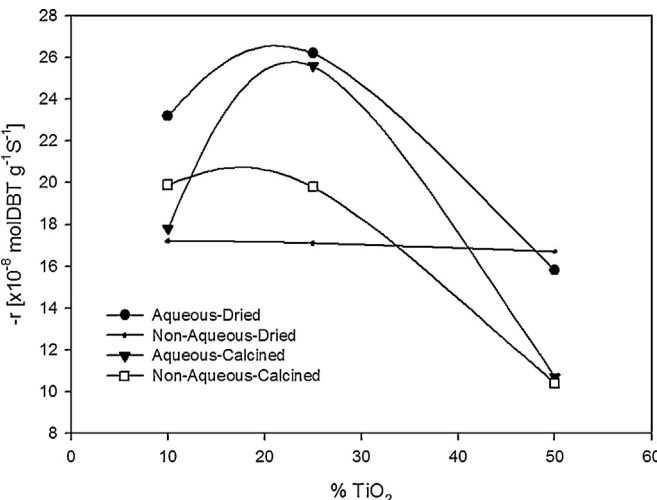


Fig. 5. UV-vis diffuse reflectance spectra of supports and dried NiW/ $\text{MgO}-\text{TiO}_2$ catalysts.

Fig. 6. UV-vis diffuse reflectance spectra of supports and calcined NiW/MgO-TiO₂ catalysts.**Table 3**

Activity and selectivity for the dried NiW catalysts impregnated by aqueous method in the DBT HDS at 593 K.

| Catalyst ^a | Initial reaction rate ($\times 10^{-8}$ mol _{DBT} s ⁻¹ gcat ⁻¹) | Selectivity (%) ^b | |
|------------------------------------|--|------------------------------|-------------------|
| | | Biphenyl | Cyclohexylbenzene |
| NiW/MT10-AD | 23.2 | 82 | 18 |
| NiW/MT25-AD | 26.2 | 70 | 30 |
| NiW/MT50-AD | 15.8 | 70 | 30 |
| NiW/Al ₂ O ₃ | 42.3 | 28 | 72 |

^a Samples were pre-activated by ex situ sulfidation.^b The selectivity is given at @15% of DBT conversion.Fig. 7. Activity of NiW/MgO-TiO₂ catalysts in HDS of DBT at 593 K.

direct desulfurization instead of hydrogenation as the commercial catalyst.

3.3. High resolution transmission electron microscopy for sulfided NiW catalysts

The catalytic activity differences between catalysts suggested some differences between the Ni and W sulfided species. HRTEM characterization for the sulfided NiW catalysts was performed in order to obtain more information about the dispersion of catalytically active WS₂ species. Fig. 8A shows HRTEM micrograph obtained from the dried NiW catalysts impregnated by aqueous method on MgTi25 support. The typical fringes of WS₂ crystallites with 0.61 nm interplanar distances were observed in all sulfided

Table 4HRTEM statistical analysis for the sulfided NiW catalysts. Average slab length (L); average stacking degree (N) and estimated f_w fraction [39].

| Sulfided catalyst | L | N | f_w |
|-------------------|------|------|-------|
| NiW/MT10-AD | 6.18 | 2.35 | 0.38 |
| NiW/MT25-AD | 3.87 | 2.30 | 0.59 |
| NiW/MT50-AD | 4.18 | 2.47 | 0.59 |
| NiW/MT10-NAC | 5.05 | 1.66 | 0.32 |
| NiW/MT25-NAC | 3.88 | 1.58 | 0.41 |
| NiW/MT50-NAC | 4.34 | 1.53 | 0.35 |

catalysts. Statistical analysis of the average stacking and length of WS₂ crystallites are shown in Fig. 8A. In general WS₂ particles observed in the catalysts were low-stacked, with a few stacks of five and six layers. The content of TiO₂ did not noticeably modify the stacking degree. However, the average length of the crystallites showed the following trend: NiW/MT10 > NiW/MT50 > NiW/MT25. The average length of the catalyst NiW/MT25-AD was 3.87 nm.

Fig. 8B shows a typical HRTEM micrograph observed in the calcined catalysts impregnated by non-aqueous method on MT10 support. Unlike catalysts previously mentioned in this work, these solids showed a very few stacks of five and four slabs, Fig. 8B. Furthermore, they did not show stacks of six slabs. These results agree with those obtained in the HDS activity, the catalyst NiW/MT50-AD shows the highest average stack, thus promoted the displacement of selectivity to the hydrogenation pathway. So it seems that the addition of TiO₂ decreased the interaction metal–MgO, however, this cannot be concluded from the results obtained in this work and requires more research in the future.

Based on Kasztelan's geometrical model [39], the average length and number of layers were used to estimate the fraction of tungsten atoms (f_w) on the edge surface of WS₂ crystallites (Table 4). This fraction changes in the following order: NiW/MT10-NAC < NiW/MT50-NAC < NiW/MT10-AD < NiW/MT25-NAC < NiW/MT50-AD ≈ NiW/MT25-AD. Thus, the aqueous

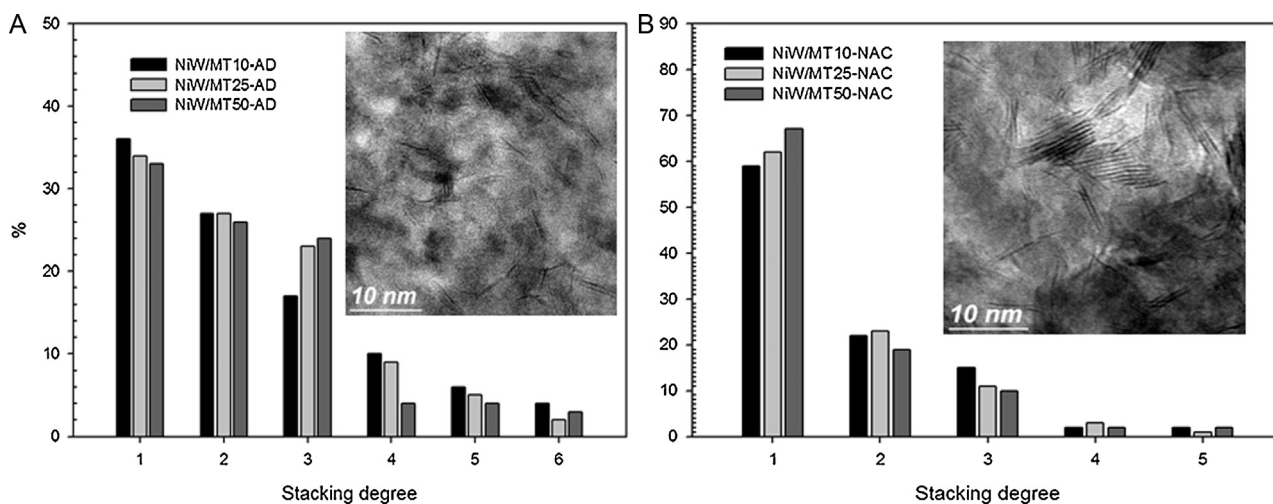


Fig. 8. HRTEM micrograph and stacking of WS₂ crystallites in sulfided (A) dried NiW catalysts impregnated by aqueous method and (B) calcined NiW catalysts impregnated by non-aqueous method.

impregnation on MgO-TiO₂ with 25 mol% of TiO₂, followed by drying at 120 °C leads to the formation of a greater number of catalytically active sites available for interaction with DBT molecules.

Many different effects could be discussed in order to explain these results, it is well known that pH and metal concentration of an impregnating solution and zero point of charge (ZPC) of the carrier are related to the amount and surface structure of supported metal oxides. The deposition of the hydroxide species over the surface is affected for the gradual solvent elimination. In the case of aqueous solution only the HW₆O₂₁⁵⁻ [40,41] and the Ni(H₂O)₆²⁺ [42] hydroxide species are present at our impregnation conditions. As the solubility of the salt is different depending on media, the formation of other surface species may be occur when the solvent was changed to methanol. (NH₄)₆W₁₂O₃₉·H₂O solubility is very low, however species W species react rapidly with the MgO of the support [43]. W ions are retained on the surface strongly and this reaction stops when surface is saturated by W species. These W-MgO close interactions may diminish their availability to form the active phases NiWS.

On the other hand, when the samples are calcined the impregnated HW₆O₂₁⁵⁻ species form the WO_x particles that are wide recognized to form strong metal-oxygen bonding. After this process the catalysts are subjected to another thermal treatment at high temperature (400 °C) in presence of H₂/H₂S in order to obtain the active phase (NiWS). When samples are only dried and then sulfided, the impregnated HW₆O₂₁⁵⁻ species form directly the active phase.

It is not possible to establish a specific reason why the maximum activity was obtained with this MT25 support. Nevertheless under the evidence presented in this manuscript and especially the results of HRTEM analysis, it is possible to suggest that the maximum in HDS activity observed in the NiW/MT25-AD catalyst is related to the morphology displayed by the WS₂ active phase in this sample as well the increase on the textural properties (117 m² g⁻¹). The average slab length (L) and stacking degree (N) in this sample resulted 3.87 and 2.30 respectively. With these parameters the fraction of W atoms in the edge of slabs were obtained resulting in the highest f_w values (0.59) among series. As example the same f_w value of 0.59 was obtained for the sample NiW/MT50-AD nevertheless the surface area fall until 36 m² g⁻¹, in this case the distribution not the dispersion was affected and therefore the catalytic activity decrease 40% compare to NiW/MT25-AD catalyst. Finally it has to be considered that a decrease on the interaction between Ni and support

could led a higher quantity of Ni atoms available to promote the WS₂ active phase.

4. Conclusions

From the activity measurements of NiW/MgO-TiO₂ catalysts in the HDS reaction of DBT and their characterization results, it was concluded that the non-aqueous method impregnation used in this study and calcination process do not improve the activity of NiW/MgO-TiO_{2(x)} catalysts. Since the NiW/MT25-NAD catalyst showed the largest number of active sites available for reaction with molecules DBT, the maximum HDS activity obtained by this solid can be explained in terms of the morphology displayed by the WS₂ active phases and the improvement of textural properties. Although the results presented in this study do not explain the interaction of Ni and W with Mg, it is possible that the addition of Ti in some way diminishes the strong interaction Metal-Mg and promotes the catalytic activity.

Acknowledgements

To project CONACyT-117373 for the financial support. To E. Aparicio, F. Ruiz, for their expert technical assistance.

References

- [1] M. Beller, A. Renken, R.A. van Santen, *Catalysis. From Principles to Applications*, Wiley-VCH, 2012.
- [2] A. Stanislaus, A. Marafi, M. Rana, *Catal. Today* 153 (2010) 6.
- [3] H. Topsøe, B.S. Clausen, F.E. Massot, *Hydrotreating Catalysis: Science and Technology*, Springer-Verlag, Berlin, Heidelberg, 1996.
- [4] J. Ramírez, S. Fuentes, G. Díaz, M. Vrinat, M. Breysse, M. Lacroix, *Appl. Catal.* 52 (1989) 211.
- [5] Pines, *The Chemistry of Catalytic Hydrocarbon Conversions*, Academic Press, New York, 1981.
- [6] T. Klicpera, M. Zdrrazil, *J. Catal.* 206 (2002) 314–320.
- [7] K.V.R. Chary, H. Ramakrishna, K.S.R. Rao, G.M. Dhar, P.K. Rao, *Catal. Lett.* 10 (1991) 27–34.
- [8] A. Pei-Hsin Yu, E.C. Myers, *Catalysis for selective hydrodesulfurization*. Standard Oil Company, UK Patent Application GB 2 017 743 A, 10 October 1979.
- [9] B. Caloch, S. Mohan, J. Rana, Ancheyta, *Catal. Today* 98 (2004) 91.
- [10] Trejo, Mohan S. Rana, J. Ancheyta, *Catal. Today* 130 (2008) 327.
- [11] T. Klímová, D.S. Casados, J. Ramírez, *Catal. Today* 43 (1998) 135–146.
- [12] S. Housseenbay, E. Payen, S. Kasztelan, J. Grimblot, *Catal. Today* 10 (1991) 541.
- [13] A. Guevara Lara, A.E. Cruz-Pérez, Z. Contreras-Valdez, J. Mogica Betancourt, A. Álvarez-Hernández, M. Vrinat, *Catal. Today* 149 (2010) 288–294.
- [14] J.M.M. Llorente, V. Rives, P. Malet, F.J. Gil-Llambias, *J. Catal.* 135 (1992) 1–12.
- [15] E. Hillerová, Z. Vit, M. Zdrrazil, *Appl. Catal. A* 118 (1994) 111.

- [16] S. Kimura, E. Yasuda, H. Kim, *Tokyo Inst. Tech. Bull.* 117 (1973) 87.
- [17] A. Nishida, S. Fukuda, Y. Kohtoku, K. Terai, *J. Ceram. Soc. Jpn.* 100 (1992) 191.
- [18] T.C. Yuan, G.V. Srinivasan, J.F. Jue, A.V. Virkar, *J. Mater. Sci.* 24 (1989) 3855.
- [19] Y.B. Lee, H.C. Park, K.D. OH, F.L. Riley, *J. Mater. Sci.* 33 (1998) 4321.
- [20] K. Tanabe, M. Misono, Y. Ono, H. Hattori, *New Solid Acid and Bases*, Kodansha, Tokyo, 1989.
- [21] M.E. Llanos, T. López, R. Gómez, *Langmuir* 13 (1997) 974.
- [22] K. Tanabe, H. Hattori, T. Sumiyoshi, K. Tanaru, T. Kondo, *J. Catal.* 53 (1978) 1.
- [23] T. López, J. Hernández, R. Gómez, X. Bokhimi, J.L. Boldú, E. Muñoz, O. Novaro, A. García Ruiz, *Langmuir* 15 (1999) 5689.
- [24] J. Ramírez, A. Gutiérrez-Alejandre, *Catal. Today* 43 (1998) 123.
- [25] O. Solcova, D.C. Uecker, U. Steinike, K. Jiratova, *Appl. Catal. A: Gen.* 94 (1993) 153.
- [26] H. Schaper, J.J. Berg-Slot, W.H.J. Stork, *Appl. Catal.* 54 (1989) 79.
- [27] M. Zdražil, *Catal. Today* 86 (2003) 151.
- [28] T. López, I. García Ruiz, R. Gómez, *J. Catal.* 127 (1991) 75.
- [29] M.C. Barrera, M. Viniegra, J. Escobar, M. Vrinat, J.A. de los Reyes, F. Murrieta, J. García, *Catal. Today* 133–135 (2008) 28.
- [30] A. Iribarren, G. Rodríguez-Gattorno, J.A. Ascencio, A. Medina, E. Torres-García, *Chem. Mater.* 18 (2006) 5446.
- [31] H. Jeziorski, H. Knozinger, *J. Phys. Chem.* 83 (1979) 1166.
- [32] J. Ramírez, G. Macías, L. Cedeño, A. Gutiérrez-Alejandre, R. Cuevas, P. Castillo, *Catal. Today* 98 (2004) 19.
- [33] M.C. Barrera, M. Viniegra, J. Escobar, M. Vrinat, J.A. de los Reyes, F. Murrieta, J. García, *Catal. Today* 98 (2004) 131.
- [34] J. Ramírez, L. Ruiz, L. Cedeño, V. Harle, M. Vrinat, M. Breysse, *Appl. Catal. A* 93 (1993) 163.
- [35] F. Iova, A. Trutia, *Opt. Mater.* 13 (2000) 455.
- [36] M.L. Jocono, M. Schavello, A. Cimino, *J. Phys. Chem.* 75 (1971) 1044.
- [37] S. Damyanova, A. Spojakina, K. Jiratova, *Appl. Catal. A* 125 (1995) 257.
- [38] A.E. Cruz-Perez, A. Guevara-Lara, J.P. Morales-Ceron, A. Alvarez-Hernandez, J.A. de los Reyes-Heredia, L. Massin, C. Geantet, M. Vrinat, *Catal. Today* 172 (2011) 203.
- [39] X.L. Yang, W.L. Dai, R. Gao, K. Fan, *J. Catal.* 249 (2007) 278.
- [40] G.D. Panagiotou, T. Petsi, K. Bourikas, C. Kordulis, A. Lycourghiotis, *J. Catal.* 262 (2009) 266.
- [41] A. Vurman, I.E. Wachs, A.M. Hirt, *J. Phys. Chem.* 95 (1991) 9928.
- [42] C. Lepetit, M. Che, *J. Phys. Chem.* 100 (1996) 3137.
- [43] T. Klíčpera, M. Zdražil, *Catal. Lett.* 58 (1999) 47.